COMPDYN 2011
3rd ECCOMAS Thematic Conference on
Computational Methods in Structural Dynamics and Earthquake Engineering
M. Papadrakakis, M. Fragiadakis, V. Plevris (eds.)
Corfu, Greece, 26–28 May 2011

NEAR-OPTIMAL BILINEAR FIT OF CAPACITY CURVES FOR EQUIVALENT SDOF ANALYSIS

F. De Luca[1], D. Vamvatsikos[2], I. Iervolino[1]

[1] University of Naples Federico II
Via Claudio, 21, 80125 Napoli, Italy
e-mail: {flavia.deluca, iunio.iervolino}@unina.it

[2] National Technical University of Athens
9 Heroon Polytechneiou, 15780 Athens, Greece
divamva@central.ntua.gr

Keywords: equivalent SDOF, bilinearization, static pushover, incremental dynamic analysis.

Abstract. *The bilinear approximation of force-deformation capacity curves is investigated for structural systems with non-negative-stiffness. This piecewise linear approximation process factually links capacity and demand; it lies at the core of the nonlinear static assessment procedures, and it has become part of seismic guidelines and codes, such as ASCE-41 and Eurocode 8. Despite codification, the various fitting rules, used to derive the bilinear representation, can produce highly heterogeneous results for the same capacity curve. This is especially valid for highly-curved backbones resulting from structural models with accurate representation of the initial, uncracked, stiffness or buildings characterized by a global collapse mechanism that leads to a gradual plasticization of the elements.*

The error introduced by the bilinearization of the force-deformation relationship is quantified by studying it at the single-degree-of-freedom (SDOF) level, away from any interference from multi-degree-of-freedom (MDOF) effects, thus avoiding the issue related to MDOF - SDOF approximation. Incremental Dynamic Analysis (IDA) is employed to enable a direct comparison of the actual backbones versus their bilinear approximations in terms of the spectral acceleration capacity for a continuum of limit-states, allowing a direct comparison of the results in terms of seismic performance.

Code-based procedures are found to be less than ideal wherever there are significant stiffness changes, while in general remaining relatively conservative. The practical fitting rules determined allow, instead, a near-optimal fit regardless of the details of the capacity curve shape.

1 INTRODUCTION

In the last decades, improvements in the computational capabilities of personal computers have allowed the employment of nonlinear analysis methods in many earthquake engineering problems. In this framework, nonlinear static analysis is becoming the routine approach for the assessment of the seismic capacity of existing buildings. Consequently, nonlinear static procedures (NSPs) for the evaluation of seismic performance, based on static pushover analysis (SPO), have been codified for use in practice. All such approaches consist of the same five basic steps: (a) perform static pushover analysis of the multi-degree-of-freedom (MDOF) system to determine the base shear versus (e.g., roof) displacement response curve; (b) fit a piecewise linear function (typically bilinear) to define the period and backbone of an equivalent single degree of freedom system (SDOF); (c) use a pre-calibrated R-μ-T (reduction factor – ductility – period) relationship for the extracted piecewise linear backbone to obtain SDOF seismic demand for a given spectrum; (d) use the static pushover curve to extract MDOF response demands; (e) compare demands to capacities; see [1] for example.

In fact, NSP is a conventional method without a rigorous theoretical foundation for application on MDOF structures [2], as several approximations are involved in each of the above steps. On the other hand, its main strength is to provide nonlinear structural capacity in a simple and straightforward way. Although several improvements and enhancements have been proposed since its introduction, any increase in the accuracy of the method is worth only if the corresponding computational effort does not increase disproportionately. Extensively investigated issues are the choice of the pattern considered to progressively load the structure and the implication of switching from the nonlinear dynamic analysis of a multiple degree of freedom (MDOF) system to the analysis of the equivalent SDOF sharing the same (or similar) capacity curve. Regarding the shape of the force distributions, it was observed that an adaptive load pattern could account for the differences between the initial elastic modal shape and the shape at the collapse mechanism [3, 4, 5]. Contemporarily, other enhanced analysis methodologies were proposed to account for higher mode effects and to improve the original MDOF-to-SDOF approximation [e.g., 6]. Regarding the demand side, efforts have been put to provide improved relationships between strength reduction factor, ductility, and period (R-μ-T relationships), to better evaluate the inelastic seismic performance at the SDOF level [7, 8].

One of the issues that have not yet been systemically investigated is the approximation introduced by the imperfect piecewise linear fit of the capacity curve for the equivalent SDOF. The necessity to employ a *multilinear* fit (an inexact, yet common, expression to describe a piecewise linear function) arises due to the use of pre-determined R-μ-T relationships that have been obtained for idealized systems with piecewise linear backbones. This has become even more important recently since nonlinear modeling practice has progressed towards realistic multi-member models, which often accurately capture the initial stiffness using uncracked section properties. The gradual plasticization of such realistic elements and models introduces a high curvature into the SPO curve that cannot be easily represented by one or two linear segments. It is an important issue whose true effect is often blurred, being lumped within the wider implications of using an equivalent SDOF approximation.

The investigation presented deals only with the bilinear approximation of the capacity curves and it is limited to non-softening force-deformation relationships. Although R-μ-T relationships that can capture far more complex backbones have recently appeared [9], the bilinear approach is by far the most widely employed in guidelines and literature [10 – 15]. The approach presented herein will be based on the accurate assessment of the effect of the equivalent SDOF fit on the nonlinear static procedure results. The latter can be achieved by proper

quantification of the bias introduced into the estimate of the seismic response at the level of the SDOF itself.

Incremental dynamic analysis (IDA) [16] will be used as benchmark method to quantify the error introduced by a bilinear fit with respect to the exact capacity curve of the SDOF. Figure 1a shows a typical example, where an elastoplastic backbone fit is used according to FEMA-440 [13]. While this fit approach is meant to result to an unbiased approximation in terms of seismic performance, the median IDA results of Figure 1b show the actual error that is introduced by such code-mandated fitting rules. In most cases, they lead to an unintended and hidden bias that is generally conservative. On the other hand, this bias can become unreasonably high in many situations.

Therefore three issues come out: First, develop a methodology aimed at quantifying the bias introduced by the fitting of a capacity curve; second, assess the the error introduced by the fitting rules already employed in codes and literature; third, perform a systematical investigation aimed at providing alternative fits that can reduce this discrepancy to almost a minimum. The comparison with existing approaches will function as the benchmark to evaluate the improvement introduced by the alternative fitting rules proposed.

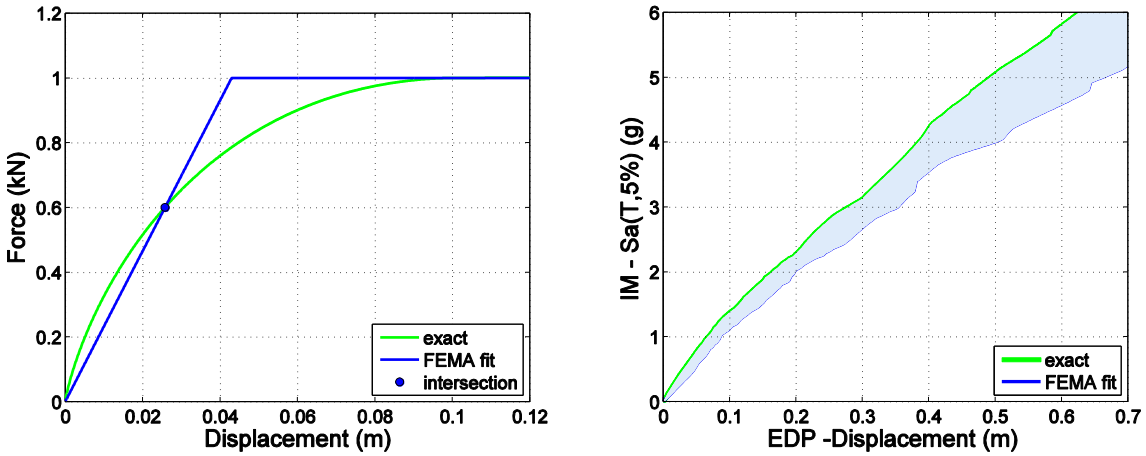

Figure 1. (a) Example of exact capacity curve versus its elastoplastic bilinear fit according to FEMA-440 and (b) the corresponding median IDA curves showing the negative (conservative) bias due to fitting for T=0.5 sec.

2 METHODOLOGY

The first main target is the quantification of the error introduced in the NSP-based seismic performance assessment by the replacement of the original capacity curve of the system, termed the "exact" or "curved" backbone, with a piecewise linear approximation, i.e., the "fitted" or "approximate" curve (e.g., Figure 1a). This will enable a reliable comparison between different fitting schemes in an attempt to minimize the observed discrepancy between actual and estimated performance. In all cases, to achieve an accurate and focused comparison of the effect of fitting only, it is necessary to disaggregate the error generated by the fit from the effect of approximating an MDOF structure via an SDOF system. Thus, all the investigations are carried out entirely at the SDOF level, using a variety of capacity curve shapes, different periods and hysteresis rules and using IDA as the method of choice for assessing the actual performance of the different alternatives.

2.1 Exact versus approximate SDOF systems

An ensemble of SDOF oscillators is considered with varying curved shapes of force-deformation backbones. They all display a monotonically decreasing stiffness that starts from elasticity and ends at a final zero or positive stiffness that remains constant for all higher deformations (e.g., Figure 1a). According to their final stiffness, these will be termed "generalized elastoplastic" and "generalized elastic-hardening" systems, respectively. They are all fitted accordingly with bilinear elastoplastic or elastic-hardening shapes.

For each considered curved backbone shape, 5% viscous damping was used and appropriate masses were employed to obtain a range of matching "reference" periods of 0.2, 0.5, 1 and 2 sec. The concept of the "reference" period, instead of the actual initial (tangent at zero displacement) period, is introduced because of the highly curved shape of some backbones. In some cases they show a strictly localized significant change in the initial stiffness, resulting in periods lower than 0.01 sec. Since this initial stiffness disappears almost immediately for any kind of loading history, a more representative reference period is required for each exact capacity curve. The reference period (T herein) was defined as the secant period at 2% of the displacement corresponding to the peak force capacity. Actually, in the vast majority of the cases there was insignificant difference between the initial tangent period and the reference secant period. In all cases, both the exact and the approximate system share the same mass, but, due to the lower initial stiffness of the latter, the "equivalent" period is equal to, or higher than, the "reference" one, thus replicating the approach followed in the conventional NSP methodology [2].

In order to draw general conclusions, independent of the hysteretic behavior assumed, two distinct hysteretic rules were considered for the each curved backbone and its bilinear fits. The first is a standard kinematic strain hardening model without any cyclic degradation characteristics. The second is a pinching hysteresis featuring cyclic stiffness degradation (see Ibarra et al [17]). When comparing an original system with its approximate having a piecewise linear backbone, the same hysteretic rules are always employed, so that both systems display the same characteristics when unloading and reloading in time-history analyses. In other words, all differences observed in the comparison can be attributed to the fitted shape of the approximate backbone; obviously also capturing any differences in the oscillator period.

For each exact shape of the SDOF's capacity curve and for each period value, several piecewise linear fit approximations have been considered according to different fitting rules. These include typical code-suggested fits, e.g., as laid out in FEMA-440 [13], ASCE/SEI 41-06 [14] and Eurocode 8 (EC8, [10]). In addition a multitude of different bilinear fits, with varying initial stiffness and yield point definition, have been employed in an attempt to pinpoint the consistent characteristics that can define an optimal or near-optimal fit. To enable a precise comparison that will allow distinguishing among relatively similar backbones in consistent performance terms, as it was previously stated, incremental dynamic analysis (IDA, [16]) will be employed.

2.2 Performance-based comparison via IDA

IDA is arguably the most comprehensive analysis method available for determining the seismic performance of structures. It involves performing a series of nonlinear dynamic analyses by scaling a suite of ground motion records to several levels of intensity, characterized by a scalar Intensity Measure (IM), and recording the structural response via one or more Engineering Demand Parameters (EDPs). The results typically appear in terms of multiple IDA curves, one for each record, plotted in the IM – EDP plane. These can be in turn summarized into the 16, 50, 84% fractile curves of EDP given IM (EDP|IM) or, equivalently (Vamvatsikos

and Cornell [18]), as the practically identical 84, 50, 16% fractile curves of IM given EDP (IM|EDP). The summarized curves thus provide the (central value and the dispersion of the) distribution of EDP seismic demand given the IM intensity of the earthquake or, vice-versa, the distribution of a structure's IM-capacity that a ground motion should exceed to achieve the given value of EDP response.

To perform IDA for each exact and approximate oscillator considered, a suite of sixty ground motion records was used, comprised of both horizontal components from thirty recordings [19] from the PEER NGA database. They are all characterized by relatively large magnitudes of 6.5 – 6.9 and moderate distances of 15 – 35km, all recorded on firm soil and bearing no marks of directivity. Using the hunt & fill algorithm [18], 34 runs were performed per record to capture each IDA curve with excellent accuracy. The IM of choice was the 5%-damped spectral acceleration at the period T of the oscillator, $S_a(T)$, while the oscillator displacement δ was used as the corresponding EDP, being the only SDOF response of interest when applying the NSP method. To avoid the appearance of arbitrary displacement scales and units, using a normalized displacement δ_n is also attractive. Unfortunately, the concise definition of a single yield point on a curved backbone is impractical, unless tied to some preselected bilinear fitting rule; therefore using some yield displacement to normalize δ to a ductility equivalent is not possible without bias. It was chosen, instead, to normalize by the value of 0.1m that signals the onset of constant stiffness in the oscillator backbone (Figure 1a).

Once the IM and EDP are decided, interpolation techniques allow the generation of a continuous IDA curve from the discrete points obtained by the 34 dynamic analyses for each ground motion record. The resulting sixty IDA curves can then be employed to estimate the summarized IDA curves for each exact and approximate pair of systems considered. Still, in order to be able to compare an exact system with reference period T with its approximation having an equivalent period T_{eq} it was necessary to have their summarized IDA curves expressed in the same IM. In this case it is chosen to be $S_a(T)$, i.e. the spectral ordinate at the period of the curved backbone oscillator. Thus, while the approximate system IDA curves are first estimated as curves in the $S_a(T_{eq}) - \delta$ (or δ_n) plane, they are now transformed to appear on $S_a(T) - \delta$ axes. This is achieved on a record-by-record basis by multiplying all 34 $S_a(T_{eq})$ values comprising the i-th IDA curve by the constant spectral ratio $[S_a(T) / S_a(T_{eq})]_i$ that characterizes the i-th record [20].

The error is evaluated for every value of displacement in terms of the relative difference between the two system median S_a-capacities, both evaluated at the reference period T of the exact system:

$$e_{50}(\delta_n) = \frac{S_{a,50}^{fit}(\delta_n) - S_{a,50}^{exact}(\delta_n)}{S_{a,50}^{exact}(\delta_n)} \tag{1}$$

Alternatively, one could use the relative error in the median displacement response given the level of spectral acceleration:

$$e_{50}(S_a) = \frac{\delta_{n,50}^{fit}(S_a) - \delta_{n,50}^{exact}(S_a)}{\delta_{n,50}^{exact}(S_a)} \tag{2}$$

Similarly, the same definitions can be used to estimate the errors for different response or capacity fractile values, e.g., 16% or 84%, or even for the dispersion in response or capacity, which, assuming lognormality, can be defined as one half the difference between the corresponding 84% and 16% values. Thus, two different ways of measuring the discrepancy between IDA curves are available, e.g., the two median IDA curves shown in Figure 1b. In one case "horizontal statistics" are employed, working with the median EDP given IM, and in the

other case "vertical statistics" of IM given EDP. As Vamvatsikos and Cornell [18] have shown, the median IDA curve is the same, regardless of how it is calculated, while, as discussed earlier, the 16, 84% fractiles are simply flipped. In addition, while there might be differences in the error estimates using these two different methods, these are only an issue of scale. Figures 2a, 2b compare the two error quantification methods for the median IDAs shown in Figure 1b. The observed trends are actually the same, but simply inverted: obviously, an overestimation in response becomes an underestimation in capacity and vice-versa.

Why then should one method be preferred over the other? There are three important reasons that make the IM-based method (IM|EDP) a more attractive solution. First, parameterizing the error in terms of the displacement response simplifies its visualization as displacement is directly mapped to specific regions of the oscillator force-deformation backbone. Thus, it is possible to see directly in Figure 2b whether the elastic or the post-elastic part is causing the accumulation of error, when it is compared vis-à-vis Figure 1a. Figure 2a is much more difficult to understand, especially if more complex backbones, than the ones used here, are considered. Second, comparing on the basis of Sa-capacity is actually directly linked to comparing in terms of the seismic performance, as expressed by the mean annual frequency (MAF) of violating limit-states defined by the oscillator displacement (Vamvatsikos [21]). An over/under-estimation of Sa-capacity maps to a consistent (although not commensurable) under/over-estimation of the MAF of limit-state exceedance. Finally, when collapse enters the problem it is obvious that the error in displacement may easily become infinite when at a given intensity level one system has collapsed, showing infinite response, while the other has not. In fact, on the contrary, this is never a problem for the Sa-based error. Although only non-collapsing systems, whose backbones never drop to zero strength, are used herein, this is another compelling reason to recommend the Sa-based comparison for general use.

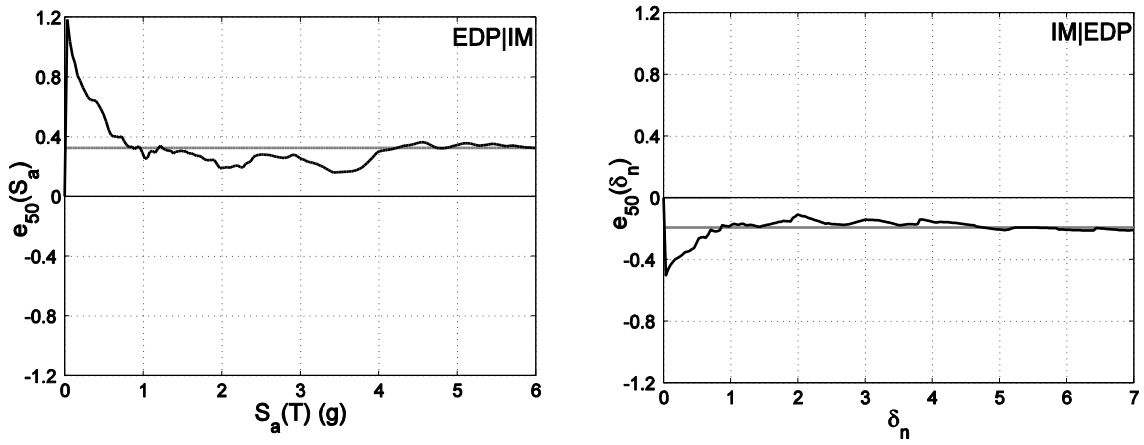

Figure 2. The relative error in the median (black line) shown versus the overall average (grey line) as introduced by the bilinear fit in Figure 1. It is expressed on the basis of (a) response given intensity (EDP|IM) and (b) intensity given response (IM|EDP).

3 INVESTIGATION OF BILINEAR FITS

Bilinear elastic-plastic or elastic-hardening fits are the fundamental force-deformation approximations employed in all NSP guidelines. The simplicity of the bilinear shape means that the only need is to estimate the position of the nominal "yield point" and select a value for the constant post-elastic stiffness. Eurocode 8 [10] suggests a piecewise bilinear fit based on the equivalence of the area discrepancy above and below the fit, assuming an elastic-plastic idealized backbone for the equivalent SDOF. This approach is similar to the original N2 method

[2]. As a consequence, EC8 prescribes an R-μ-T relationship [7] based on the elastic-perfectly-plastic fit. FEMA documents [11, 12, 13] gradually upgraded the proposed piece-wise linear fit by integrating rules to account for softening behavior. According to FEMA 356 [12], the idealized relationship is bilinear with an initial slope and a post yield slope evaluated by balancing the area above and below the capacity curve up to the target displacement and calculating the initial effective slope at a base shear force equal to 60% of the nominal yield strength. The proposed graphical procedure is iterative. FEMA 440 [13] and ASCE/SEI 41-06 [14] assume the basic approach of FEMA 356 with additional rules regarding the softening behavior. In the following pages only non-softening capacity curves (generalized elastic-plastic or elastic-hardening) are investigated, thus in essence it is the original FEMA 356 and the EC8 fit rules that are tested.

In order to develop an improved bilinear fit, we choose to investigate separately the fitting of the initial "elastic" segment and then focus on the post-elastic non-negative stiffness part. Thus, we will first study generalized elastic-plastic systems, where the stiffness becomes zero beyond a displacement of 0.10 m and the target displacement is assumed to be well into the fully plastic region. Thus the post-elastic segment is fixed to have zero stiffness while the initial "elastic" part can be fitted at will. In both the FEMA and EC8 fitting rules, the fitted "elastic" stiffness can be a function of the target displacement due to the area balancing used. This can make the bilinear fitting yield different results depending on the limit-state of interest and may initially put the code-mandated fits (as implemented herein) at a slight disadvantage. It will be remedied in the second part of the study where generalized elastic-hardening systems will be tackled. They have varying post-yield stiffness and lower target displacements, allowing more fitting flexibility and providing a more rigorous comparison of code fits against any proposal for a near-optimal fit. Generally, the target, herein, is the development of a simple fitting rule that performs well for a continuum of limit states. Therefore, the performance of all rules will be carefully examined even outside the immediate region of interest defined by a target displacement.

3.1 Bilinear fits of generalized elastic-plastic systems

First a family of generalized elastic-plastic capacity curves is considered that exhibit a stiffness gradually decreasing with deformation, starting from the initial elastic and reaching zero slope. The shapes are characterized by the magnitude of the changes in stiffness. Figure 3a and 3b give an example of the shapes employed in the investigation of this family of backbones and emphasize two opposing cases. The first (Figure 3a) is not characterized by significant curvature, while the second (Figure 3b) shows a significant change in slope that can be representative of the behavior of a model that accounts for uncracked stiffness. Both the kinematic strain hardening and the pinching hysteresis are considered.

Three basic fitting rules are compared: (a) the FEMA fit (60% rule) assuming a target displacement high enough so that the slope of the second branch of the bilinear can be assumed to be zero; (b) the EC8 fit using a simple equal area criterion; (c) the "10% fit", defined so that the intersection between the capacity curve and the fitted elastic segment is at 10% of the maximum base shear. The latter is the proposal for a simple rule that can better capture the initial stiffness. Figure 3a shows that in the case in which the capacity curves are not characterized by significant stiffness changes at the beginning of the backbone, the three fits are very similar to each other. They differ significantly though when the initial backbone stiffness diminishes rapidly, as in Figure 3b. In all cases the fitted post-elastic stiffness is set to zero.

As described in the previous section, IDA is performed for each of the SDOF systems presented in Figure 3 and their fitted approximations for a range of periods. Figures 4 and 5 show

the comparison in the median Sa-capacity for T equal to 0.2 and 0.5 sec, respectively. Obviously, the shapes of the backbones have a significant impact. In all cases, the error becomes significant for the shape with non-trivial curved segments. In both cases though, the maximum error appears at the earlier backbone segments. Curiously, the 10% fit leads to a remarkable decrease in the error for any deformation level, even for the highly curved shape of Figure 3b where it clearly violates any notion of equal area (or equal energy) that seems to be prevalent in current guidelines. The new fit introduced leads to a slightly non-conservative estimation of the capacity for displacements before the full plasticization (for δ_n up to 1) and only for short-period systems, T = 0.2 sec (Figure 4). On the other hand, even in case of highly-curved backbones (Figure 4b) only a 10% underestimation appears at most. On the contrary, it has to be noted that code approaches are always conservative for all the displacement levels and all the shapes considered, but at a cost of almost 20 – 40% underestimation of capacity. The trends identified are generally confirmed for all other periods considered (T equal to 1.0 and 2.0 seconds).

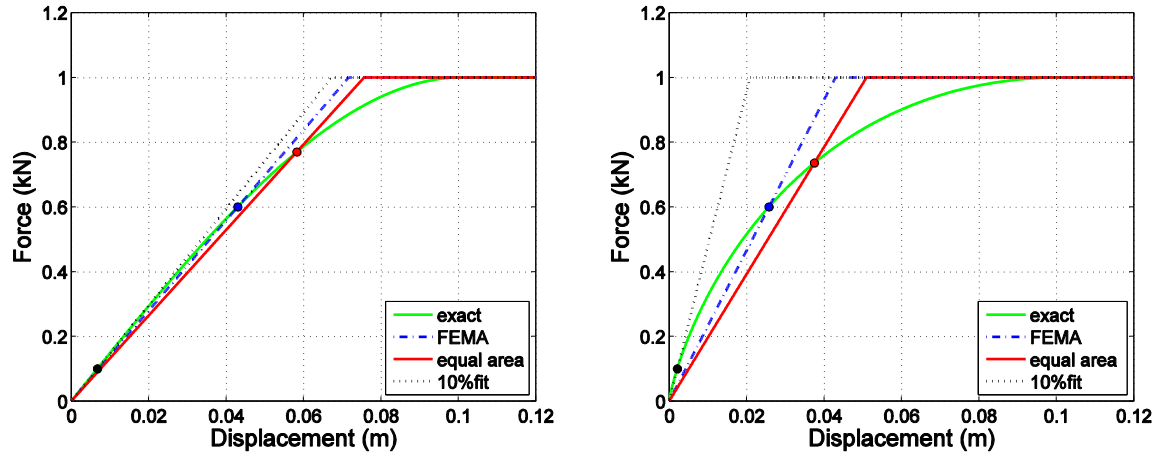

Figure 3. Comparison of generalized elastic-plastic capacity curves and their corresponding fits having (a) insignificant versus (b) significant changes in initial stiffness.

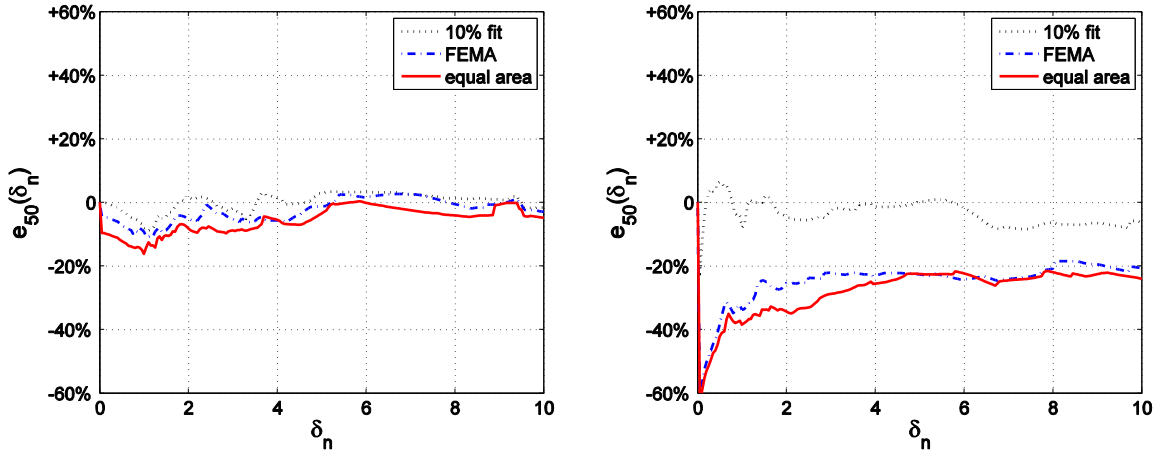

Figure 4. Median relative error comparison between the 10%, FEMA and equal area fits for T = 0.2 sec, when applied to the capacity curves of Figure 3: (a) insignificant versus (b) significant changes in initial stiffness.

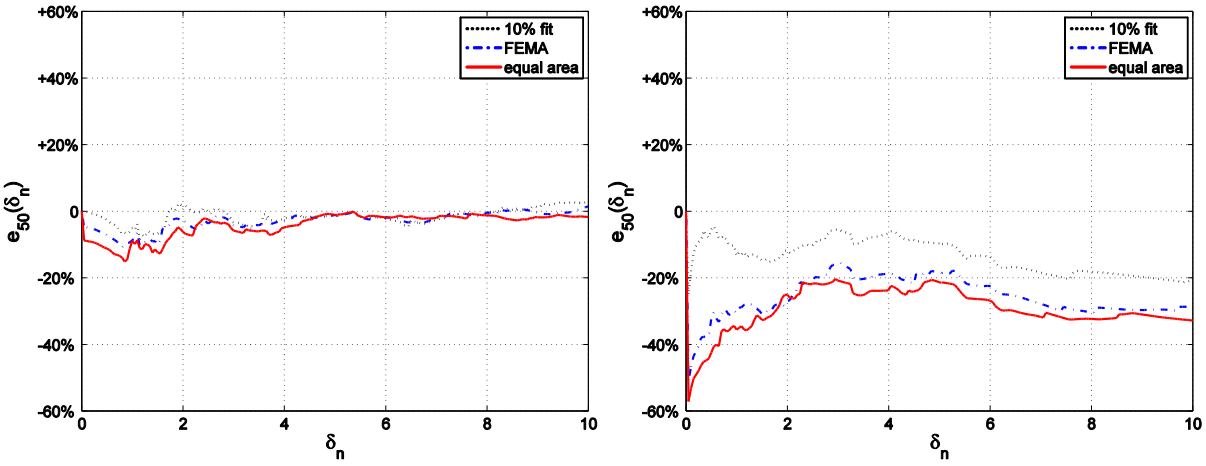

Figure 5. Median relative error comparison between the 10%, FEMA and equal area fits for T = 0.5 sec, when applied to the capacity curves of Figure 3: (a) insignificant versus (b) significant changes in initial stiffness.

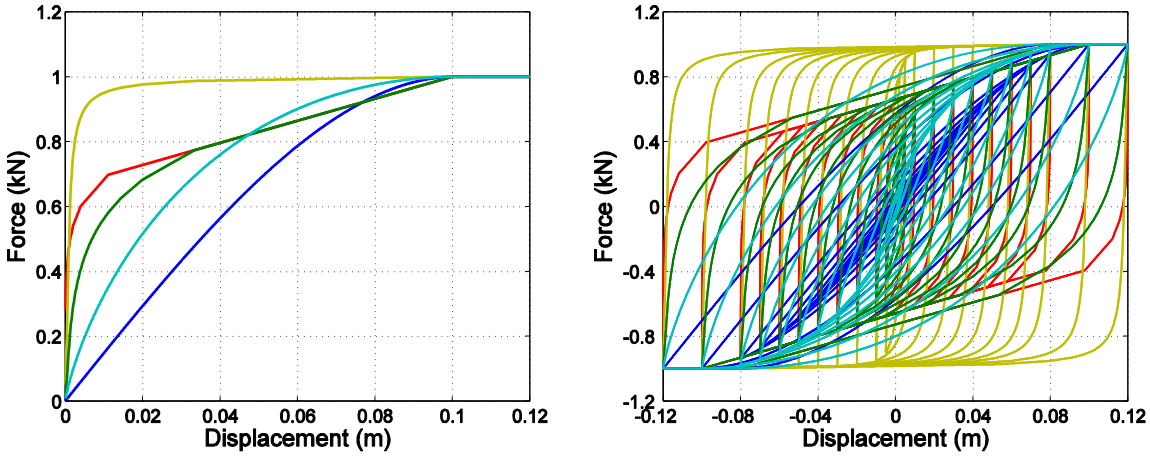

Figure 6. (a) Backbones and (b) hysteretic behavior according to standard kinematic strain hardening rule of the generalized elastic-plastic systems considered.

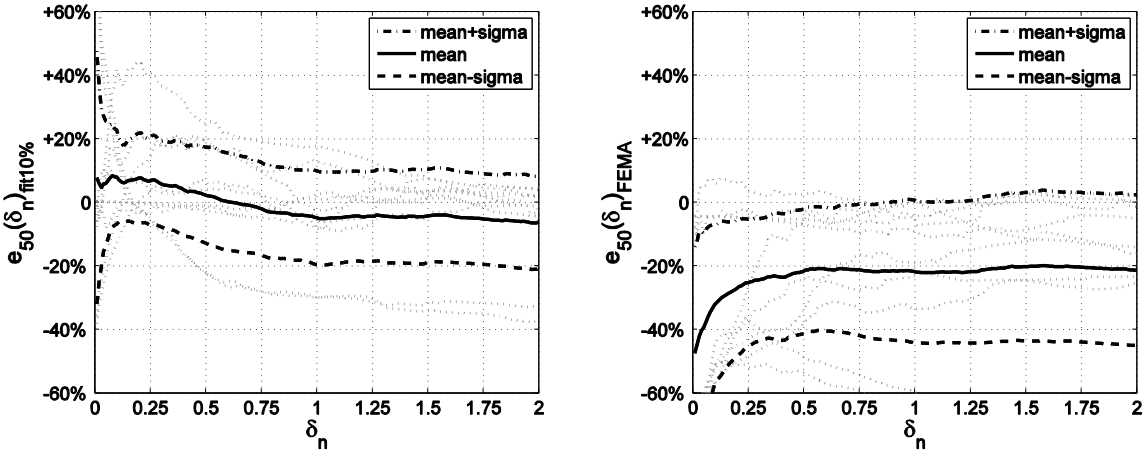

Figure 7. The median relative error for (a) the 10% fit and (b) the 60% FEMA fit, T = 0.2 sec, in case of elastic-plastic SDOF system family (grey dotted lines).

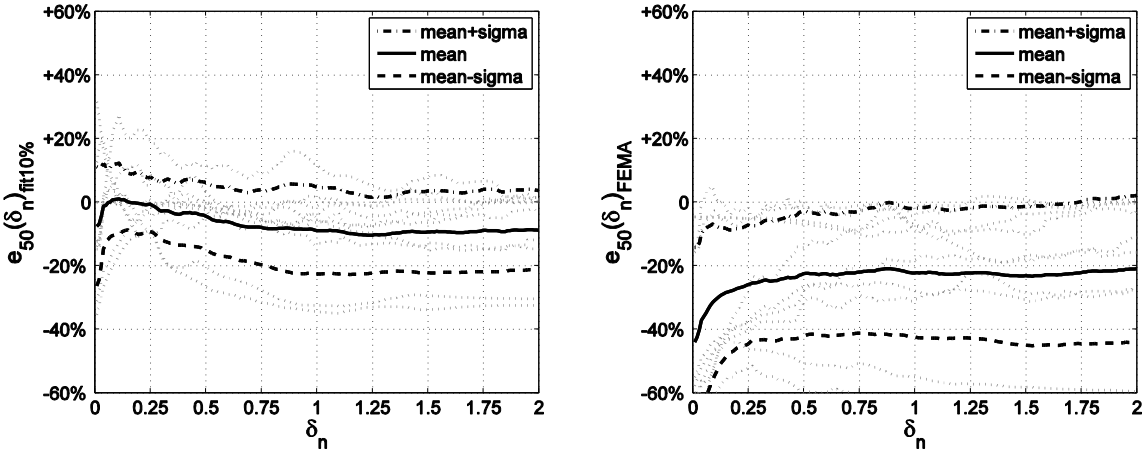

Figure 8. The median relative error for (a) the 10% fit and (b) the 60% FEMA fit, T = 0.5 sec, in case of elastic-plastic SDOF systems family (grey dotted lines).

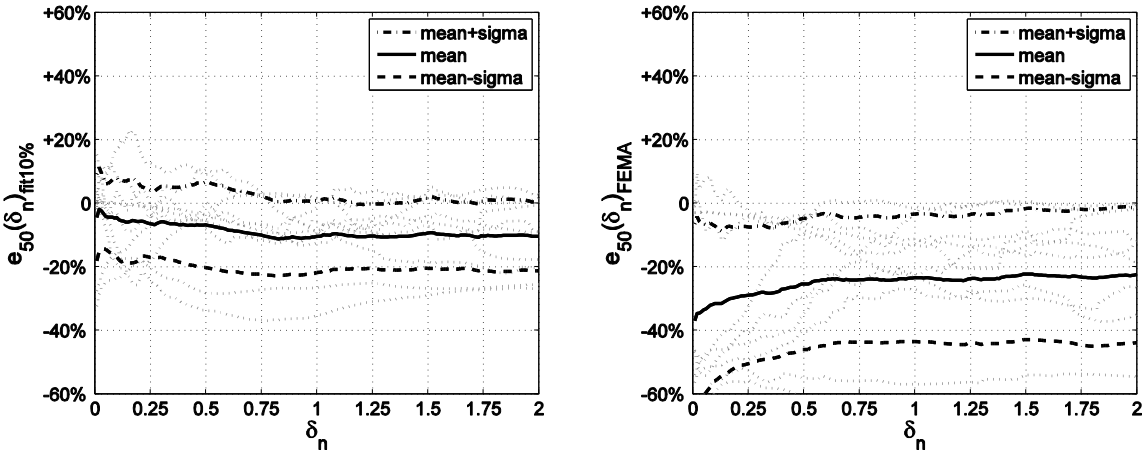

Figure 9. The median relative error for (a) the 10% fit and (b) the 60% FEMA fit, T = 1.0 sec, in case of elastic-plastic SDOF systems family (grey dotted lines).

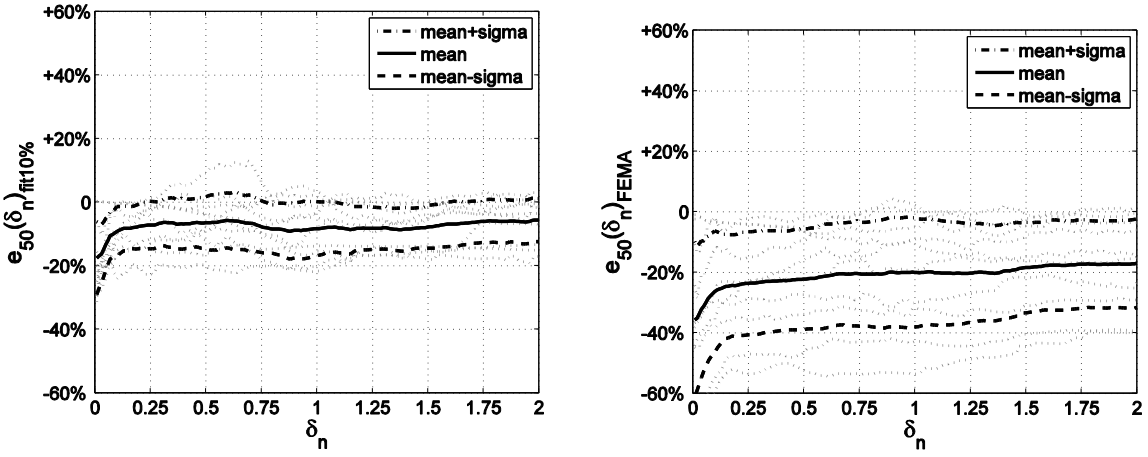

Figure 10. The median relative error for (a) the 10% fit and (b) the 60% FEMA fit, T = 2.0 sec, in case of elastic-plastic SDOF systems family (grey dotted lines).

Beyond the two curved shapes shown in Figures 3a, b, a number of different generalized elastic-plastic shapes were also investigated A sample of ten backbones is considered aimed at drawing out general conclusions regarding the proposal fit investigated. The sample is consists of five different shapes (see Figure 6a) times the two hysteretic rules described in section 2. In Figure 6b the standard kinematic strain hardening rule is shown for the five shapes considered.

Figure 7 to Figure 10 show the relative error on the median S_a-capacity evaluated at each period for the 10% fit proposed and the conventional FEMA fit. The bias is evaluated up to δ_n equal to 2, where most of the significant differences appear. This is evident for the two shapes in Figure 3a and 3b where it was evaluated up to δ_n equal to 10. Figure 7 to Figure 10 show grey dotted lines representing the error related to a specific shape of the backbone and to a specific hysteretic rule. The hysteretic rule chosen was found to be insignificant, as the error depends primarily on the shape of the fit; thus the two different hysteretic behaviors have been considered together to build up a heterogeneous family of generalized elastic-plastic behavior.

The 10% fit enjoys an insignificant bias on average for all the periods considered and the error introduced by the fit never exceeds 20%. FEMA fits shows a strictly negative, i.e., conservative, bias of 20% or even 60%, depending on the shape of the original backbone. Most of the bias is concentrated at the beginning of the backbone as it was already emphasized by the examples in Figure 3. Error comparisons for the S_a-capacity dispersion (record to record) are not shown as all fits roughly achieve similar performance. Some differences may appear in the region preceding the nominal yield point of the approximation. Therein the fitted system will predict no dispersion whereas the actual one shows some small variability. Still, this is to be expected and it is not important enough to make us favor one fit over another.

Summing up, it can be stated that the fit should capture as close as possible the initial stiffness of the backbone while the generally low secant stiffness assumed in most of the guidelines and codes tends to be overly-conservative. The only possible exception to this rule appears only for initially ultra-stiff systems that very quickly lose their initial properties. This is the reason why fitting the "elastic" secant at 5% or 10% of the maximum base shear, as opposed to 0.5% or 1% is considered a more robust strategy.

3.2 Bilinear fits of generalized elastic-hardening systems

The second family of shapes investigated is characterized by a generalized elastic-hardening behavior. Only the pinching hysteretic rule was considered for this family of backbones, given the insignificant differences observed earlier when compared to the kinematic hardening. Each backbone considered was characterized by different curvatures and final hardening stiffness, allowing a wide coverage of the typical shapes that can be obtained considering different structural behaviors and modeling options.

In analogy with the two examples showed in the previous subsection, two different backbones will be presented in detail from the family considered. The first (Figure 11a) is not characterized by significant changes in the stiffness, in contrast to the second (Figure 11b). The target displacement is assumed to be equal to 0.2 m. The EC8 fit is not applied as it is restricted to elastic-plastic approximations which are clearly inferior for the shapes shown in Figure 11. On the other hand, the FEMA fit rule can be applied without problems, although it might call for different approximations depending on the value of the target displacement. Still, the results and the corresponding conclusions remain the same in all cases. The alternative fit proposed, termed the "H-10%" rule, determines the initial stiffness at 10% (instead of 60%) of the nominal yield shear defined in accordance with FEMA, while the post-elastic

stiffness is determined by minimizing the absolute area discrepancy between the capacity curve and the fitted line. The area minimization leads to similar results as the balancing of areas above and below the fitted line. While easy to apply graphically, the latter is an ill-defined problem that can yield mixed results: Imagine two coincident equal-size linear segments where one, the "approximation", is rotated by an arbitrary angle around the common center. Obviously, the rotated segment always satisfies the area balancing rule as a valid approximation to the original. Only when it becomes coincident does it satisfy the minimum area criterion. Thus, area minimization is algorithmically superior. The proposed H-10% procedure came out as the simplest rule with a near-minimum error for this family of backbones. While many alternatives were considered, they are not showed herein for the sake of brevity.

It has to be noted that elastic-plastic fits according to the proposal of the previous subsection have been also considered in the investigation of this family of backbones, assuming the plateau of the fit at the force corresponding to the target displacement (e.g. at 0.2m here); even if less performing than the H-10% rule, considered in the following, the still low bias of those trials compared to the FEMA-356 fitting rule, enforced the general conclusion that capturing the initial stiffness is the dominant criterion that leads to a significant bias reduction with respect to actual code fit prescriptions.

The results of the two fitting procedures (H-10% and FEMA-356) applied to the example shapes appear in Figure 11. Obviously, when the stiffness of the backbone is not characterized by abrupt changes in the curvature (Figure 11a) both fits tend to be practically the same. Figure 12 and Figure 13 show the error introduced by each fit, for both backbone shapes considered in Figure 11, in the cases of T = 0.2 and 0.5 sec, respectively. In analogy with the results presented for the elastic-plastic case, most of the error is concentrated at the beginning of the backbone. In the case of the backbone with low changes in the stiffness (low curvature), it can be observed that the error is very small and very similar for both fits. A higher curvature of the backbone increases the error introduced by the fit and emphasizes that although at the target displacement the backbones and their fits in both cases are coincident, this is not enough to guarantee the same error. The earlier fitted segments and especially the defined equivalent period can make a large difference. As the H-10% rule manages to capture the initial stiffness better, it provides better predictive capability for higher displacements.

The evidence, again, confirms the general trend already shown in the previous section, that it is important to capture the initial stiffness of the capacity curve to have an unbiased fit. In this case, as well, the code approach results in a conservative error that can be over 50% in the case of non-trivial shapes and at the lower displacement values (see Figure 11b). In the same range, the H-10% fit leads to a slightly non-conservative solution only for the short periods (T = 0.2 sec), an effect that was also observed in the elastic-plastic backbone family. Otherwise the fit remains conservative and overall it can be considered to be relatively unbiased.

In this case a sample of only four shapes is considered, the different shapes shown in Figure 14a and the pinching hysteretic rule assumed for this backbones appearing in Figure 14b. In Figure 15 to Figure 18 the relative errors in the median S_a-capacity, are compared for the four different periods and the different SDOF backbones. The importance of capturing the initial stiffness is highlighted by the results at each period, and the H-10% fit leads to a small and relatively unbiased error, which seldom exceeds 10%. In this case the sample of backbones considered for the elastic-hardening case was smaller than the elastic-plastic case but the robustness of the general results, showing the same trends in both cases, supports our remarks. It should be noted that the results of the FEMA approximation will improve somewhat at low displacements if we refit for a lower target displacement, but not enough to alter the above conclusions.

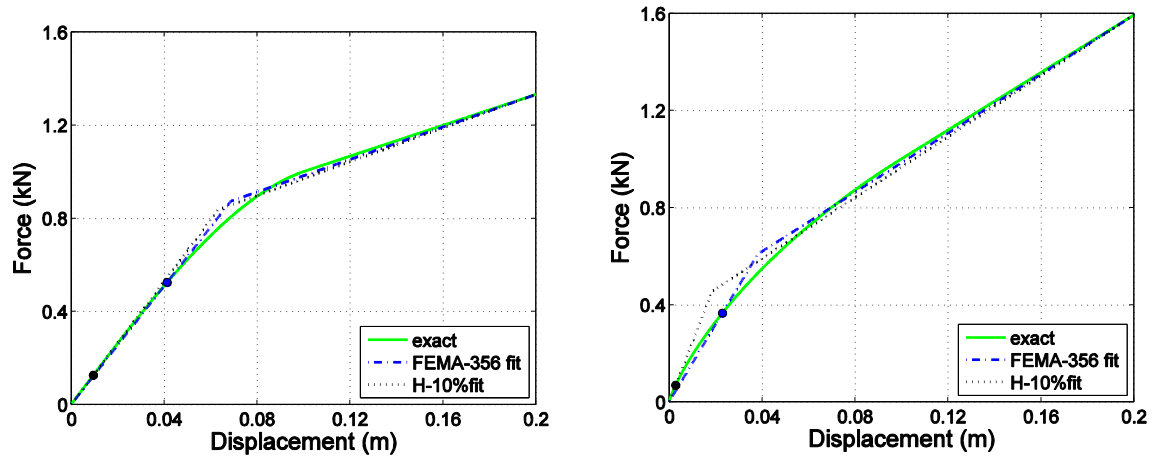

Figure 11. Comparison of generalized elastic-plastic capacity curves and their corresponding fits having (a) insignificant versus (b) significant changes in initial stiffness.

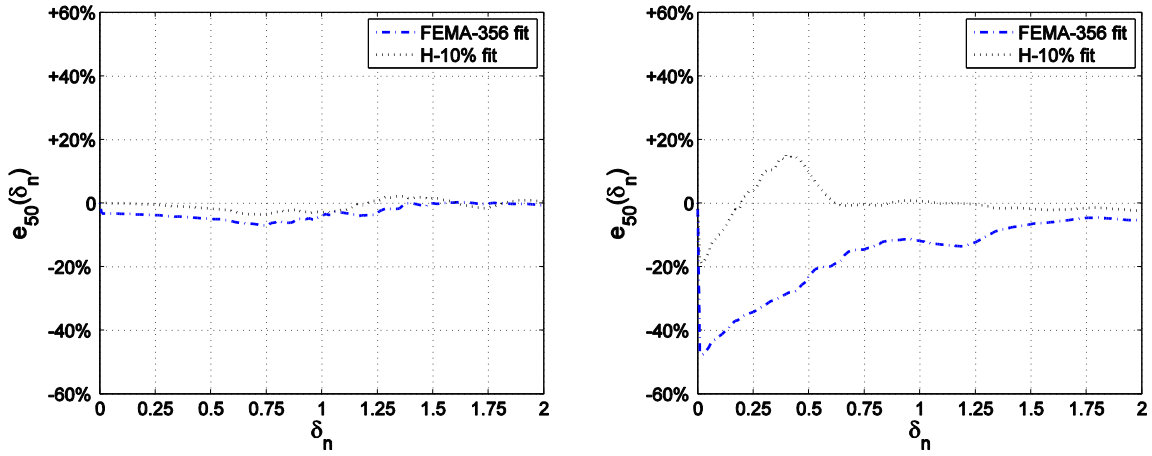

Figure 12. Median relative error comparison between the H-10% and FEMA fits for T = 0.2 sec, when applied to the capacity curves of Figure 10: (a) insignificant versus (b) significant changes in initial stiffness.

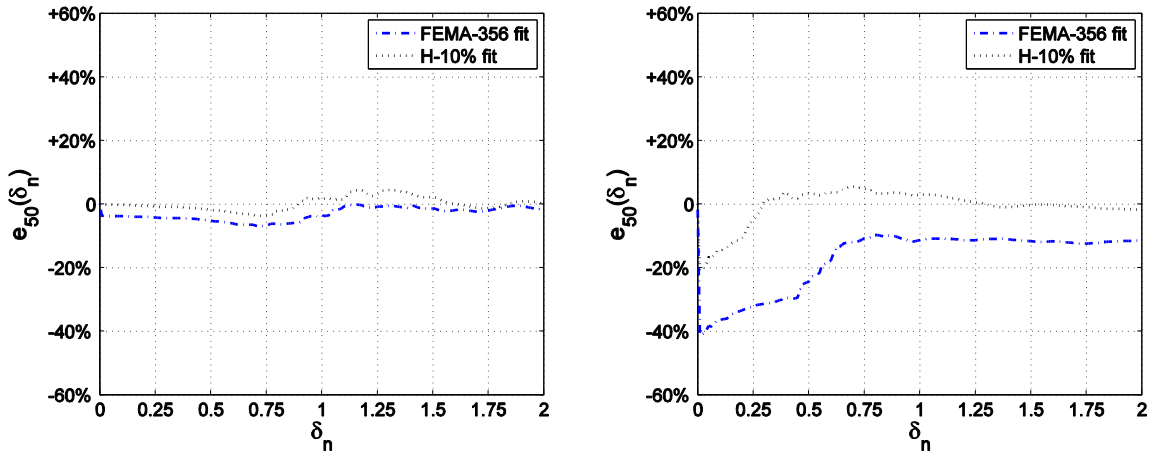

Figure 13. Median relative error comparison between the H-10% and FEMA fits for T = 0.5 sec, when applied to the capacity curves of Figure 10: (a) insignificant versus (b) significant changes in initial stiffness.

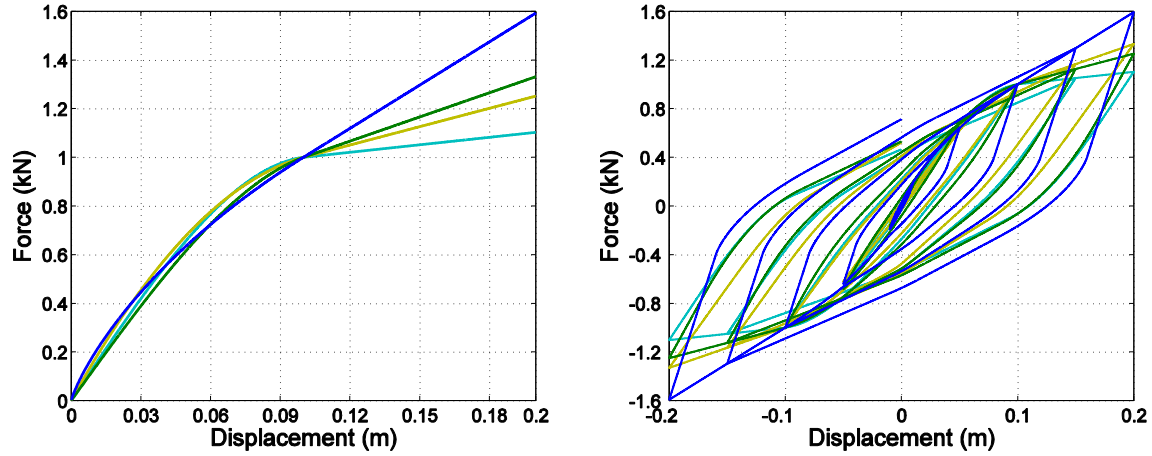

Figure 14. Backbones (a) and hysteretic behavior according to pinching hysteresis rule (b) of the generalized elastic-hardening systems considered.

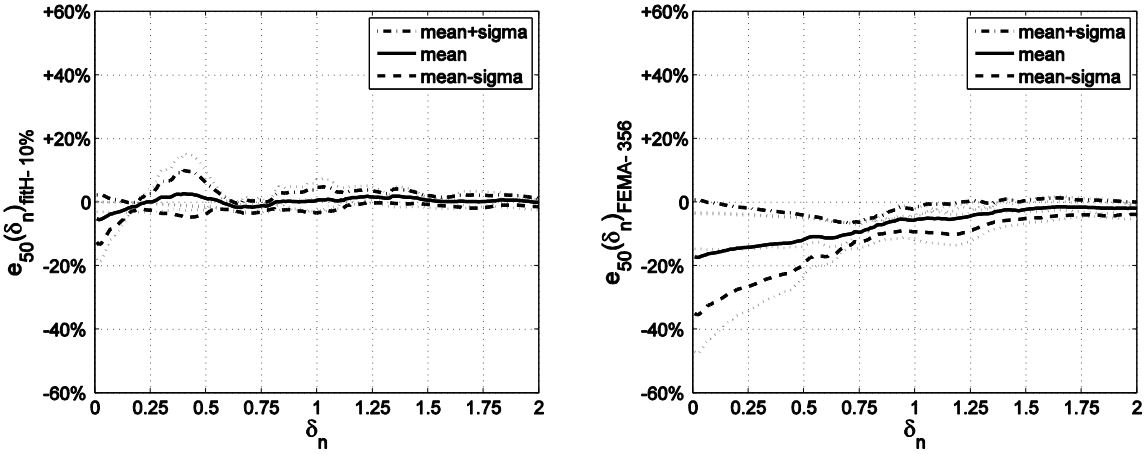

Figure 15. The median relative error for (a) the H-10% fit and (b) the 60% FEMA fit, T = 0.2 sec, in case of elastic-hardening SDOF systems family (grey dotted lines).

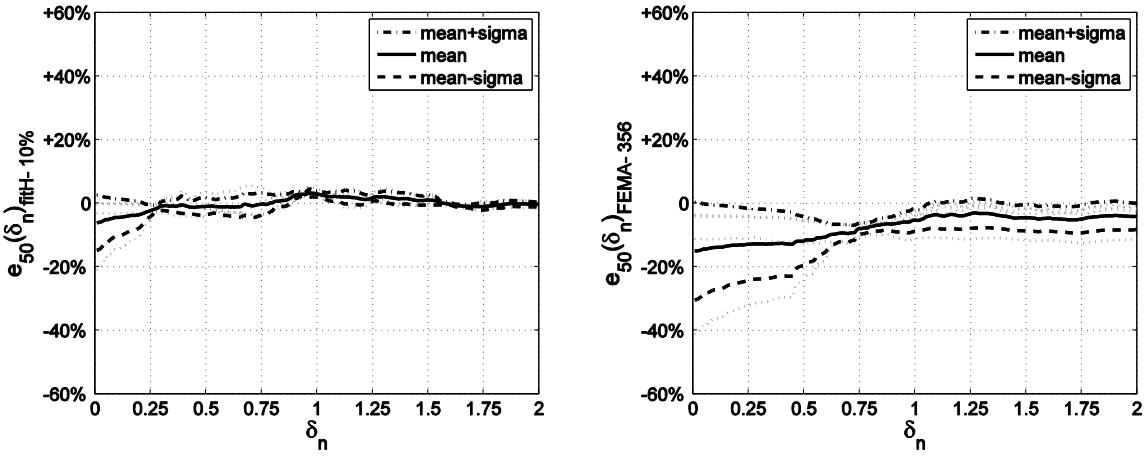

Figure 16. The median relative error for (a) the H-10% fit and (b) the 60% FEMA fit, T = 0.5 sec, in case of elastic-hardening SDOF systems family (grey dotted lines).

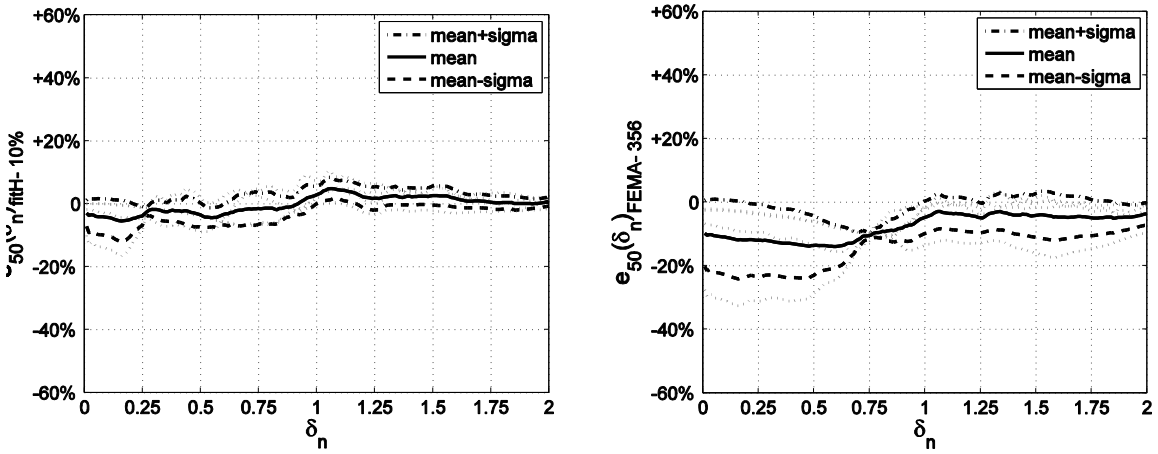

Figure 17. The median relative error for (a) the H-10% fit and (b) the 60% FEMA fit, T = 1.0 sec, in case of elastic-hardening SDOF systems family (grey dotted lines).

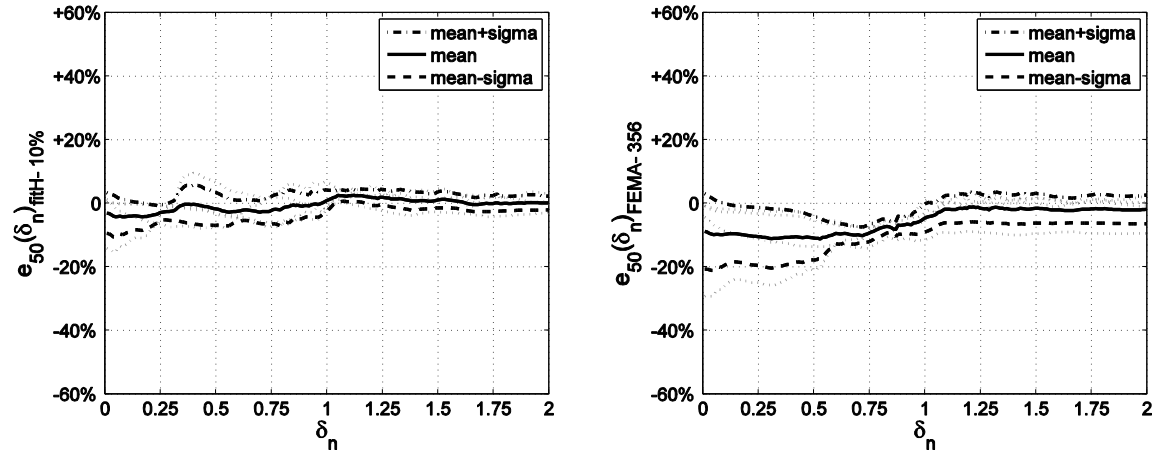

Figure 18. The median relative error for (a) the H-10% fit and (b) the 60% FEMA fit, T = 2 sec, in case of elastic-hardening SDOF systems family (grey dotted lines).

4 CONCLUSIONS

Structural seismic assessment based on the nonlinear static procedure is a method that, in its different versions, has become common in the last decades among researchers and practitioners. It is based on the fundamental approximation that the behavior of an MDOF system can be interpreted by the response of an equivalent SDOF. This necessitates a number of approximations at various stages of the procedure. Herein, the problem of the optimal bilinear fit to be chosen as the idealized base shear–displacement curve is systematically investigated by means of an IDA-based procedure applied to the case of non-softening capacity curves.

Assessment of different fits is achieved on an intensity-measure capacity basis that allows a straightforward comparison of the performance of structural systems characterized by different periods, in this case the period of the capacity curve and its bilinear approximation. Therefore the approach followed allows the investigation of a continuum of limit states at the SDOF level, excluding other sources of error that have already been investigated by other detailed studies.

The investigation led to the general rule and recommendation that it is fundamental to capture the initial stiffness of the capacity curve rather than aiming at balancing or minimizing

the area above or below the elastic segment of the fit. A 10% of a reference value of yield base shear, i.e., the maximum attained for elastic-plastic and the nominal yield value for elastic-hardening systems, is suggested as a robust point for the intersection between the capacity curve and the fit of the elastic secant segment. The subsequent non-negative stiffness segment should be chosen to minimize the area discrepancy between the fitted and the exact model in the region of interest.

The low bias introduced by this enhanced fit is found to be an improvement with respect to existing code approaches. Essentially it can be assumed to be a near-optimal solution especially in the case of capacity curves with significant changes in stiffness, representative of modern modeling approaches that account for the uncracked section properties. The error introduced by the near optimal bilinear fit does not exceed 20% for elastic-plastic fits and it seldom exceeds 10% for systems with hardening, while codified approaches were found to be generally conservative, sometimes more than 50% for highly curved shapes.

ACKNOWLEDGEMENTS

The analyses presented in the paper have been developed in cooperation with Rete dei Laboratori Universitari di Ingegneria Sismica – ReLUIS for the research program funded by the Department of Civil Protection – Executive Project 2010-2013.

REFERENCES

[1] P. Fajfar and M. Fischinger, N2 – A method for non-linear seismic analysis of regular structures. *Proceedings of the 9th World Conference on Earthquake Engineering*, Tokyo, 111-116, 1988.

[2] H. Krawinkler and G.P.D.K. Seneviratna, Pros and cons of a pushover analysis of seismic performance evaluation. *Engineering Structures*, **20**, 452-464, 1998.

[3] J.M. Bracci, S.K. Kunnath and A.M. Reinhorn, Seismic performance and retrofit evaluation of reinforced concrete structures *Journal of Structural Engineering* **123**, 3-10, 1997.

[4] A.S. Elnashai, Advanced inelastic static (pushover) analysis for earthquake applications. *Structural Engineering and Mechanics* **12**, 51-69, 2001.

[5] S. Antoniou, R. Pinho, Advantage and limitations of adaptive and non-adaptive force-based pushover procedures. *Journal of Earthquake Engineering* **8**, 497-522, 2004.

[6] A.K. Chopra and R.K. Goel, A modal pushover analysis procedure for estimating seismic demands for buildings. *Earthquake Engineering and Structural Dynamics*, **31**, 561-582, 2002.

[7] T. Vidic, P. Fajfar, M. Fischinger, Consistent inelastic design spectra: strength and displacement. *Earthquake Engineering and Structural Dynamics*, **23**, 507-521, 1994.

[8] E. Miranda and V.V. Bertero, Evaluation of strength reduction factors for earthquake-resistant design. *Earthquake Spectra*, **10**(2), 357-379, 1994.

[9] D. Vamvatsikos and C.A. Cornell, Direct estimation of the seismic demand and capacity of oscillators with multi-linear static pushovers through Incremental Dynamic Analysis. *Earthquake Engineering and Structural Dynamics*, **35**(9), 1097-1117, 2006.

[10] Comitè Europèen de Normalisation. *Eurocode 8 – Design of Structures for earthquake resistance – Part 1: General rules, seismic actions and rules for buildings*. EN 1998-1, CEN, Brussels, 2003.

[11] Federal Emergency Management Agency (FEMA), *NEHRP Guidelines for the seismic rehabilitation of buildings*. Report No. FEMA-273, Washington, D.C., 1997.

[12] Federal Emergency Management Agency (FEMA), *Prestandard and commentary for the seismic rehabilitation of buildings*. Report No. FEMA-356, Washington, D.C., 2000.

[13] Federal Emergency Management Agency (FEMA), *Improvement of nonlinear static seismic analysis procedures*. Report No. FEMA-440, Washington, D.C., 2005

[14] American Society of Civil Engineers (ASCE), *Seismic Rehabilitation of Existing Buildings*, ASCE/SEI 41-06, Reston, Virginia, 2007.

[15] S.W. Han, K. Moon, A.K. Chopra, Application of MPA to estimate probability of collapse of structures. *Earthquake Engineering and Structural Dynamics*, **39**, 1259-1278, 2010.

[16] D. Vamvatsikos and C.A. Cornell, Incremental Dynamic Analysis. *Earthquake Engineering and Structural Dynamics*, **31**, 491-514, 2002.

[17] L.F. Ibarra, R.A. Medina, H. Krawinkler, Hysteretic models that incorporate strength and stiffness deterioration, *Earthquake Engineering and Structural Dynamics*, **34**, 1489-1511, 2005.

[18] D. Vamvatsikos and C.A. Cornell, Applied Incremental Dynamic Analysis. *Earthquake Spectra*, **20**, 523-553, 2004.

[19] D. Vamvatsikos, M. Fragiadakis, Incremental dynamic analysis for estimating seismic performance sensitivity and uncertainty. *Earthquake Engineering and Structural Dynamics*, **39**, 141-163, 2010.

[20] M. Fragiadakis, D. Vamvatsikos, M. Papadrakis., Evaluation of the influence of vertical irregularities on the seismic performance of a nine-storey steel frame. *Earthquake Engineering and Structural Dynamics*, **35**, 1489-1509, 2006.

[21] D. Vamvatsikos, Some thoughts on methods to compare the seismic performance of alternate structural designs. In: Dolsek M. (ed), *Protection of Built Environment Against Earthquakes*. Springer: Dordrecht, 2011.